Supporting Information (SI) for: Microsecond Carrier Lifetimes, Controlled p-Doping and Enhanced Air Stability in Low-Bandgap Metal Halide Perovskites

Alan R. Bowman[1], Matthew T. Klug[2], Tiarnan A. S. Doherty[1], Michael D. Farrar[2], Satyaprasad P. Senanayak[1], Bernard Wenger[2], Giorgio Divitini[3], Edward P. Booker[1], Zahra Andaji-Garmaroudi[1], Stuart Macpherson[1], Edoardo Ruggeri[1], Henning Sirringhaus[1], Henry J. Snaith[2*] & Samuel D. Stranks[1*]

1. Cavendish Laboratory, Department of Physics, University of Cambridge, JJ Thomson Avenue, Cambridge, CB3 0HE, UK
2. Department of Physics, University of Oxford, Clarendon Laboratory, Parks Road, Oxford, OX1 3PU, UK
3. Department of Materials Science and Metallurgy, University of Cambridge, 27 Charles Babbage Road, Cambridge, CB3 0FS, UK
*Corresponding authors: sds65@cam.ac.uk, henry.snaith@physics.ox.ac.uk

Experimental methods
Fabrication

Materials

Formamidinium iodide (FAI) was purchased from Greatcell Solar. Lead (II) iodide (PbI_2, 99.999 % Ultradry), tin (II) iodide (SnI_2, 99.999 % Ultradry), zinc iodide (ZnI_2, 99.995 % Ultradry) was purchased from Alfa Aesar. Tin (II) fluoride (SnF_2, 99 %), lead (II) thiocyanate (99.5 %, $Pb(SCN)_2$), anisole (anhydrous 99.7 %), *N,N*-dimethylformamide (DMF, anhydrous ≥99.8 %), dimethyl sulfoxide (DMSO, anhydrous ≥99.9 %), chlorobenzene (CB, anhydrous 99.8 %) was purchased from Sigma Aldrich. Poly(3, 4-ethylenedioxythiophene)-poly(styrenesulfonate) (PEDOT:PSS, PVP AI 4083) was purchased from Heraeus. Methanol (MeOH) was purchased from Fischer Scientific.

Perovskite solution preparation

A stoichiometric 0.75 M solution of $FAPb_{0.5}Sn_{0.5}I_3$ was prepared in a nitrogen atmosphere by dissolving FAI, PbI_2, and SnI_2 in a mixed solvent of 3:1 DMF:DMSO by volume with an additional amount of SnF_2 (20 % molar amount with respect to SnI_2) and $Pb(SCN)_2$ (6 % molar amount with respect to PbI_2). A stoichiometric 0.75 M solution of $FAZnI_3$ was also prepared in a nitrogen atmosphere by dissolving FAI and ZnI_2 in a mixed solvent of 3:1 DMF:DMSO. The solutions were stirred at room temperature and filtered with a 0.45 μm PTFE filter prior to use. The $FAPb_{0.5}Sn_{0.5}I_3$ and $FAZnI_3$ solutions were blended to achieve the desired $FA(Pb:Sn:Zn)I_3$ ratio.
We define x = (concentration of ZnI_2 in precursor solution)/0.75 M, where 0.75 M is the concentration of FAI in all precursor solutions. i.e.

x=	FAI concentration (M)	PbI_2 concentration (M)	SnI_2 concentration (M)	ZnI_2 concentration (M)
0 %	0.75	0.375	0.375	0
2 %	0.75	0.3675	0.3675	0.015
5 %	0.75	0.35625	0.35625	0.0375
10 %	0.75	0.3375	0.3375	0.075

For solar cells a 0.8M solution concentration was used with the solvent quench method and a solvent mix of 4:1 DMF:DMSO, which was found to be more optimal for solar cells.

Films for characterisation

Films for photoluminescence and transient absorption spectroscopy measurements were prepared on O2-plasma treated glass substrates (O_2-plasma treatment lasted for 10 minutes). The perovskite layer was deposited by statically spin-coating 120 μL of the 0.75 M $FA(Pb:Sn:Zn)I_3$ solution at 5 krpm for 30 s with a 6 s ramp. At 14 s into the spin-coating program, a stream of compressed N_2 gas was applied to the spinning film for 16 s. After spinning is finished, the substrate was annealed at 100 °C for 10 minutes. The neat perovskite films were then encapsulated (see encapsulation notes below). Films for electron microscopy and transistors were prepared on O_2-plasma treated silicon.

Solar cell fabrication

Pre-patterned indium tin oxide (ITO) substrates (Shenzhen Huayu Union Technology Co Ltd, 10 ohm/sq) were cleaned via sonication in a diluted Hellamanex solution (1% vol in DI water), deionized water, acetone, and isopropanol sequentially for 5 minutes each. The remaining isopropanol was dried off with a nitrogen gun. Substrates were then treated with an O2 plasma process for 10 minutes prior to spinning the PEDOT:PSS layer.
Poly(3,4-ethylenedioxythiophene) polystyrene sulfonate (PEDOT:PSS; Clevios P VP Al 4083, aqueous dispersion) solutions were prepared by diluting the as received PEDOT:PSS dispersion in MeOH in a 1:2 ratio respectively. Films were deposited on ITO (Indium Tin Oxide) via a static dispense of 180 µL followed by spinning at 4000 rpm for 40 seconds and subsequently annealed for 10 min at 150 ^{o}C.
Perovskite films were fabricated by spin coating and the solvent quench method in a nitrogen filled glovebox. This resulted in shorter lifetimes but still increased resistance to air with ZnI_2 (see Figure S11). 100 µL of precursor solution was statically dispensed onto the substrate and the liquid meniscus was pulled over the substrate using the pipette tip. The substrate was spun at 3600 rpm for a total of 30 s. At 13 s 200 µL of anisole was pipetted onto the middle of the spinning substrate with a dispense time of around 1 s. As soon as the chuck stopped a steady stream of nitrogen via a nitrogen gun was applied the surface of the film for a further 15 s. Films were annealed at 100 ^{o}C for 10 minutes.
PCBM ([6,6]-Phenyl C61 butyric acid methyl ester, Solenne BV) solutions were prepared to a concentration of 20 mg/mL in a 3:1 mixture of chlorobenzene to dichlorobenzene. Once made solutions were left for at least 24 h at room temperature before filtering with a 0.2 µm PTFE filter. PCBM was dynamically spin coated on top of the perovskite layer at 2000 rpm using 50 µL of solution and annealing for 1 minute at 100 ^{o}C .
BCP (Bathocuproine, Sigma Aldrich) solutions were prepared to a concentration of 0.5 mg/ml in isopropanol. Solutions were stirred overnight at 70 °C and then filtered a 0.2 µm PTFE filter prior to use. BCP was dynamically spin coated on top of the perovskite layer at 5000 rpm using 70 µL of solution (with no annealing).
All electrodes for devices were deposited using a shadow mask to give an electrode pattern complimentary to the solar simulator used. The pattern resulted in 8 pixels per substrate each with an active area of 0.0919 cm^2. A Kurt J. Lesker Nano 36 evaporator was used to deposit Ag electrodes. This final step resulted in ~1 minute of air exposure prior to electrode deposition.

Encapsulation

Samples for optical characterization were encapsulated in a solvent-free, nitrogen-filled glovebox immediately following encapsulation (within ~10 minutes of end of annealing). First a 25 x 25 mm perovskite-coated glass substrate was broken into quarters and thin strips of Kapton tape were applied to the edges of a quarter-substrate sample to act as a spacer layer to disrupt thin-film interference effects (only in the case of TAS measurements). An 18 mm x 18 mm glass cover slip was then placed on top of the sample and a UV-curable resin (5 second UV Light Fix, Ontel products) was applied to the corner between the side edges of the glass quarter-substrate and the underside of the oversized cover-slip. The sample was sealed one edge at a time by applying the resin and curing with a UV LED for 10 seconds (peak wavelength 400 nm). Once all edges were sealed, the whole sample was illuminated with a UV light for 5 minutes. To ensure the encapsulation was not altering the samples one encapsulation was carried out with a quick drying two part epoxy (Evo-Stik Rapid, Bostik Ltd.) and similar PLQE and TCSPC results were obtained.

Spectroscopy

Photoluminescence quantum efficiency

PLQE measurements were recorded using an integrating sphere, following the three measurement approach of De Mello et al.[1] A continuous wave temperature controlled 647 nm laser was used to photo excite samples (Thorlabs). The emission was recorded using an Andor IDus DU490A InGaAs detector. Spot size was recorded using a Thorlabs beam profiler, where the size was set to be to where the intensity of the beam falls to $1/e^2$. The equivalent 1 sun level was found by calculating the absorbed flux of photons from the AM1.5 spectrum using measured absorbance ($\int AM1.5(E)a(E)dE$) and using a laser excitation power to achieve the same absorbed flux of photons.

Time correlated single photon counting

Time-resolved PL measurements were acquired using a time-correlated single photon counting (TCSPC) setup (FluoTime 300 PicoQuant GmbH). Film samples were photoexcited using a 635 nm laser head (LDH-P-635, PicoQuant GmbH) pulsed at a frequency of 0.2 MHz, with a pulse duration of 73 ps and fluence of ~50 $nJcm^{-2}$. The PL was collected using a high resolution monochromator and near infra-red photomultiplier detector assembly (NIR PMT, H10330A, Hamamatsu). Spot size was measured by recording transmitted power while the beam was partially blocked by a razor blade. This blade was slowly translated to allow for transmission of more of the beam and the distance of travel recorded. Transmitted power versus distance was fitted by a Gaussian beam profile[2] and the beam size defined to be to the point where the intensity falls by $1/e^2$.

To remove the encapsulation a sharp razor blade was taken to the edge of the encapsulant with the cover slip placed on a worktop. Pressure was slowly increased until the encapsulation came free and the sample exposed to air. Care was taken to ensure that there were no marks on the perovskite material.

Transient absorption spectroscopy

For the pump, sub-ns pulses were generated by a frequency doubled q-switched Nd:YVO_4 laser (AOT-YVO-25QSPX, Advanced Optical Technologies). A Spectra Physics Solstice Ti:Sapphire laser generated 90 fs pulses at a frequency of 1 kHz and a broad band probe beam was generated using a home-built noncollinear optical parametric amplifier. Probe and reference beams were measured with a Si dual-line array detector (Hamamatsu S8381-1024Q) and read by a board from Stresing Entwicklungbüro (custom made). Other details are similar to those in Rao et al.[3] Spot size was recorded using a Thorlabs beam profiler, where the size was set to be where the intensity of the beam falls to $1/e^2$.

Electrical characterisation

Transistors

Bottom gate bottom contact perovskite field effect transistors were fabricated using Si/SiO_2 substrate on which Au source drain electrodes are lithographically patterned. Perovskite thin films were spin coated using the same technique as above. All devices were characterized in a vacuum chamber (10^{-6} mbar) using an Agilent 4155B parameter analyser operated in pulsed mode for transfer characteristics and continuous mode for output characteristics. For the

transfer characteristics performed using the pulsed mode a short impulse of 0.5 ms corresponding to V_g was applied and the measurements were performed under continuous V_d. For the photo-illumination study the device was illuminated from the top with an intensity controllable white light source which reaches a maximum intensity of 10 mW/cm^2. The interfacial charge density is estimate from the threshold voltage (V_{th}) value obtained from the transfer curves using the expression: $Q = C (V_g - V_{th})/e$, where C is the capacitance per unit area of the SiO_2 layer, V_g is the maximum gate voltage and e is the unit of electronic charge. Photoinduced charge is then estimated from the difference in interfacial charge between the dark and the photoinduced transfer measurements. As control experiments we fabricated device with only ZnI_2 layer and transistor characterization was also performed.

Solar Cell Testing

Current-voltage (JV) characteristics of the solar cells were recorded in ambient air under simulated AM1.5 solar light (1-Sun, 100 mW cm-2) generated by an ABET Class AAB sun 2000 simulator. The solar simulator was calibrated for low-bandgap perovskite materials with bandgaps around 1.2 eV by using a certified KG2 filtered silicon reference cell to correct for spectral mismatch. Each device was measured with a 20 mV voltage step and a 100 ms time step (i.e. scan rate of 0.2 V/s) using a Keithley 2400 source meter. All devices were masked with a 0.0919 cm^2 metal aperture to define the active area and eliminate edge effects. Stabilised power output (SPO) measurements were performed by holding the device at the voltage of the maximum power point, as determined by the JV characteristic, and monitoring the current density over the course of 60 s.

Structural characterisation

Scanning transmission electron microscopy energy-dispersive X-Ray Spectroscopy

An FEI Helios Nanolab dual beam Focused Ion Beam/ Field Emission Gun – Scanning Electron Microscope (FIB/FEGSEM) was employed to prepare a lamella for STEM imaging and analysis. Thin films deposited on both PEDOT and Si were examined. A capping layer of Spiro-OMeTAD was deposited on top of both films to prevent damage and aid in charge transport during the FIB process. Pt was deposited on top of the Spiro- OMeTAD in the region of interest prior to FIB milling of the electron transparent lamella from the bulk sample. The lamella was immediately transferred to an FEI Tecnai OSIRIS STEM equipped with a high brightness Schottky X-FEG gun and a Super-X EDX system composed by four silicon drift detectors, each approximately 30 mm^2 in area and placed symmetrically around the optic axis achieving a collection solid angle of 0.9 sr, where STEM/EDX data was acquired. Spectrum images were recorded at an acceleration voltage of 200 kV, a spatial sampling of 10 nm/pixel and a 100 ms/pixel dwell time. All data was acquired with Tecnai Imaging Analysis (TIA) and analysed with Hyperspy[4].

Scanning electron microscopy

Images in Figure S1 were generated using a field-emission scanning electron microscope (FESEM, Merlin). A thin layer of platinum was sputtered on the surface of the sample on silicon wafers before SEM imaging. An electron beam accelerated to 3 kV was used with an in-lens detector.

For images in Figure S12 a Hitachi S-4300 was used, using an electron beam accelerated at 5kV. In these images no platinum sputtering was used prior to imaging.

Atomic force microscopy

Sample thickness was recorded using an Asylum Research MFP-3D atomic force microscope in non-contact AC mode. A scratch on the surface on an unencapsulated sample was made using metal tweezers and the average difference in height between the material surface and the glass below as recorded (after 0^{th} order flattening and 1^{st} order plane fit were applied). All measurements and data processing were carried out on Asylum Research AFM Software version 15.

X-Ray diffraction

XRD was performed using a Bruker X-ray D8 Advance diffractometer with Cu Kα1,2 radiation (λ= 1.541 Å). Spectra were collected with an angular range of $10° < 2\theta < 45.7°$ and $\Delta\theta = 0.02044°$ over 30 minutes. Measurements were made on both as prepared spin coated films. The Bruker Topas software[5] was used to carry out Le Bail[6] on a single crystal sample over an angular range of $10° < 2\theta < 45.7°$. Backgrounds were fit with a Chebyshev polynomial function and the peak shape modelled with a pseudo-Voigt function.

SI Note 1

Relationship of the ground state bleach to the number of excited charges

The absorption coefficient as a function of transition frequency, $\alpha(\omega)$, can be defined as[7]

$$\alpha(\omega) = \frac{\pi c \mu e^2}{n \omega m^2} |\mathrm{M}|^2 \rho(\epsilon)(f(\epsilon_j) - f(\epsilon_i))$$

Here c is the speed of light in a vacuum, μ the magnetic permeability, e the charge of an electron, n the refractive index, m the mass of an electron, M the matrix element of the transition, $f(\epsilon_i)$ the probability that state ϵ_i is occupied, ϵ_j the lower energy state, ϵ_i the upper energy state (so $\epsilon = \hbar\omega = \epsilon_i - \epsilon_j$) and $\rho(\epsilon)d\epsilon$ is the number of states that lie between $\hbar\omega$ and $\hbar\omega + d\epsilon$.
We can also define the number of electrons in the conduction band, n, and the number of holes in the valence band, p, of a semiconductor as

$$n = \int_{E_c}^{\infty} n(\epsilon, \mu_c) g_c(\epsilon) d\epsilon$$

$$p = \int_{-\infty}^{E_v} g_v(\epsilon)(1 - n(\epsilon, \mu_v))\, d\epsilon$$

where $n(\epsilon, \mu)$ is the probability of occupation at energy ϵ with chemical potential μ, g_i is the density of states of the valence (v) or conduction (c) band respectively and E_i is the energy at the top of the valence/bottom of the conduction band. If we assume parabolic bands close to the bottom of the conduction band and the top of the valence band (e.g. $\epsilon_c = \epsilon_{c,0} + \frac{\hbar^2 k_c^2}{2m_c}$), and note that for a direct optical transition there must be no momentum change upon absorption/emission ($k_c = k_v \equiv k$), then it is straightforward to show that $g_c(\epsilon), g_v(\epsilon) \propto k$, the wavevector. We also note that

$$\rho(\epsilon) = \frac{k^2}{\pi^2 \left(\left(\frac{d\epsilon_i}{dk}\right) - \left(\frac{d\epsilon_j}{dk}\right) \right)}$$

using the relationship between energy levels for a direct optical transition is $\epsilon_i(k) = \epsilon_j(k) + h\omega$. Noting the parabolic band assumption, it can be shown that $\rho(\epsilon) \propto k \propto g_c(\epsilon), g_v(\epsilon)$. Therefore, the absorption coefficient can be re-written as

$$\alpha(\omega) = (A g_v(\epsilon_j) n(\epsilon_j, \mu_v) - B g_c(\epsilon_i) n(\epsilon_i, \mu_c))$$

where A and B are constants whose difference depends on the relative effective masses of electrons and holes.

The signal recorded in transient absorption spectroscopy is

$$\frac{\Delta T}{T} \approx \frac{e^{-t\alpha_{excited}} - e^{-t\alpha_{unexcited}}}{e^{-t\alpha_{unexcited}}}$$

assuming that the reference signal is the same shot to shot, where *t* is the sample thickness. Assuming that the change in absorption coefficient is small,

$$\frac{\Delta T}{T} = -A' g_v(\epsilon_j)\Delta n(\epsilon_j, \mu_v) + B' g_c(\epsilon_i)\Delta n(\epsilon_i, \mu_c)$$

Integrating about the bandgap (i.e. around the ground state bleach) we obtain

$$\int_{\lambda\, min}^{\lambda\, max} \frac{\Delta T}{T} d\lambda = A'' n_{ex}(t) + B'' p_{ex}(t).$$

SI Note 2

Initial excitation density

We calculate the initial excitation density, n_0, using

$$n_0 = \frac{aP}{f\hbar\omega\pi\left(\frac{d}{2}\right)^2 t}$$

Here *a* is the fraction of light absorbed by the film (as measured by UV-VIS spectroscopy), *P* the power of the beam, *f* the repetition rate of the laser, *d* the diameter of the Gaussian beam (defined as $\frac{1}{e^2}$) and *t* the thickness of the film, as measured using atomic force microscopy.

SI Note 3

Extraction of background hole concentration from PLQE measurements

Photoluminesence quantum efficiency can be modelled as

$$PLQE = \frac{\eta_{esc} b_r (p_0 n + n^2)}{an + bn(n + p_0) + cn^3}$$

and in a continuous wave measurement the generation rate is

$$G = an + bn(n + p_0) + cn^3.$$

Here η_{esc} is the probability an emitted photon escapes the film, b_r is the radiative rate, p_i is the background hole concentration, n the excited carrier concentration and a, b and c decay rates measured in TA.

a, b and *c* are known from TA so *n* can be calculated for a steady state measurement. By plotting $\frac{PLQE*G}{n}$ versus n we obtain a straight line with gradient of $\eta_{esc} b_r$ and intercept equal to $\eta_{esc} b_r p_0$. The ratio of these two values gives us an estimate of p_0. Results are given in table S2 and fitting shown in figure S9. It should be noted that to avoid effects of sample heating during measurement, we carried out this fitting on our PLQE data using only the low carrier concentration region (i.e. $n < 1{\times}10^{16} cm^{-3}$).

SI Note 4

As discussed in the main text, it is possible to achieve reasonable efficiencies for Pb-Sn perovskites solar cells without encapsulating devices, while our spectroscopic data (Figure 1, main text) suggests that the lifetime of charges becomes negligibly small after a few minutes of air exposure. To explore this point we carried out TCSPC on a glass/perovskite(*x*=0 %)/PCBM/BCP stack with and without a silver electrode (Figure S14). The photoluminescence lifetime of stacks without silver electrodes drops to <1 ns within an hour of air exposure, while for regions covered by silver electrodes the photoluminescence lifetime remains the same following 17 hours of air exposure (between measurements samples were stored in a desiccator). Furthermore, by illuminating a region of the stack with an electrode, but in a region not covered by the electrode (due to a mask during silver evaporation) we confirm that the silver is providing protection from air: in this region the lifetime had again fallen to <1 ns following 17 hours of air exposure.

Table S1

Excitation fluence ($nJcm^{-2}$)	*Time for signal to fall to $\frac{1}{e}$ of initial value (ns)*			
	x=0 %	*x=2 %*	*x=5 %*	*x=10 %*
50	*360*	*510*	*490*	*160*
33	*530*	*610*	*550*	*190*
17	*780*	*780*	*740*	*240*
5	*1520*	*1170*	*1190*	*370*

The time taken for TCSPC signal to fall to $\frac{1}{e}$ of initial value for four excitation fluences for each film.

Table S2

	$MAPbI_3$ (from Richter et al.[8])	*x*=0 % films	*x*=5 % films
$a+bp_0$ (s^{-1})	5e6	1e5	3.3e5
b (cm^3s^{-1})	8.1e-11	1.1e-10	3.6e-11
c (cm^6s^{-1})	1.1e-28	3.0e-29	2.6e-28
$\eta_{esc}b_r$ (cm^3s^{-1})	9e-12	(1.8±0.2)e-12	(1.7±0.1)e-12
p_0 (cm^{-3})	0 (no observable background carriers)	<2.5e14	(1.0±0.3)e15

The decay kinetics measured for our low-bandgap perovskite films (x= 0 %, x=5 %) compared to previously recorded $MAPbI_3$, as measured using TA (for a, b and c), and an estimation of doping density from a combination of PLQE and TA (see SI note 3).

Supplementary Figures

a)

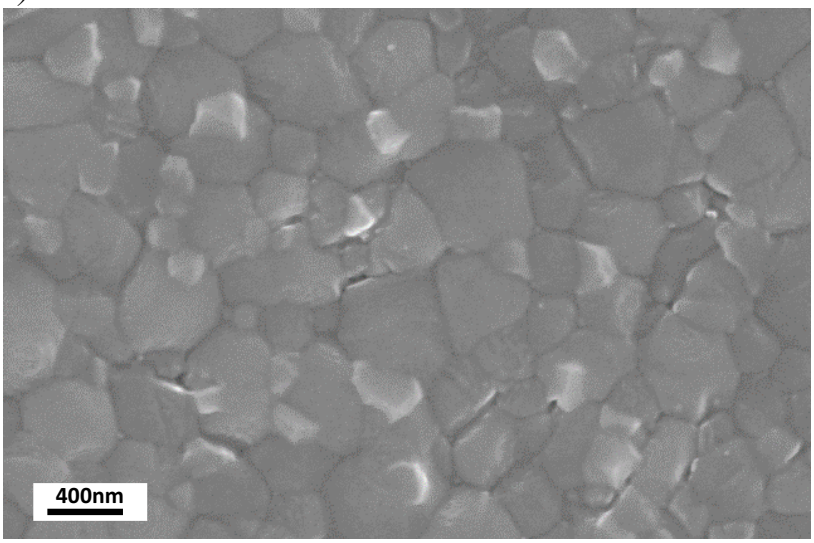

b)

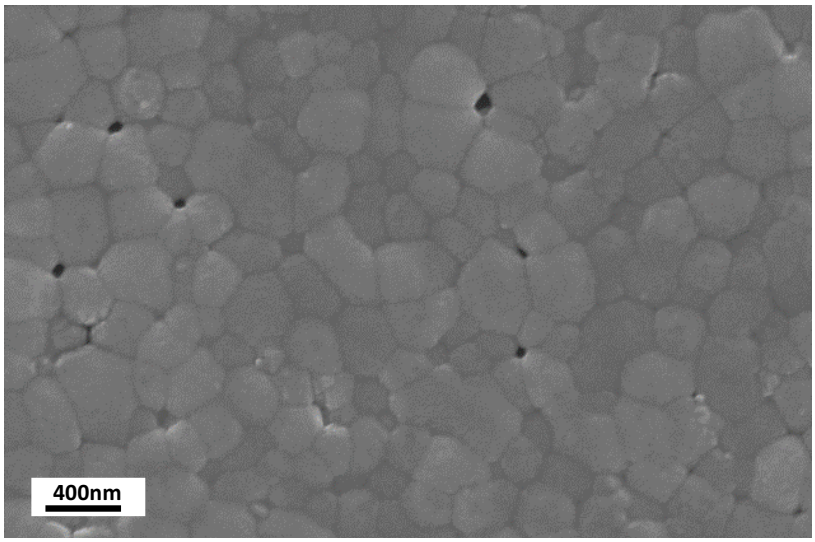

Figure S1. a) and b) SEM images for x=0 % and x=5 % films respectively.

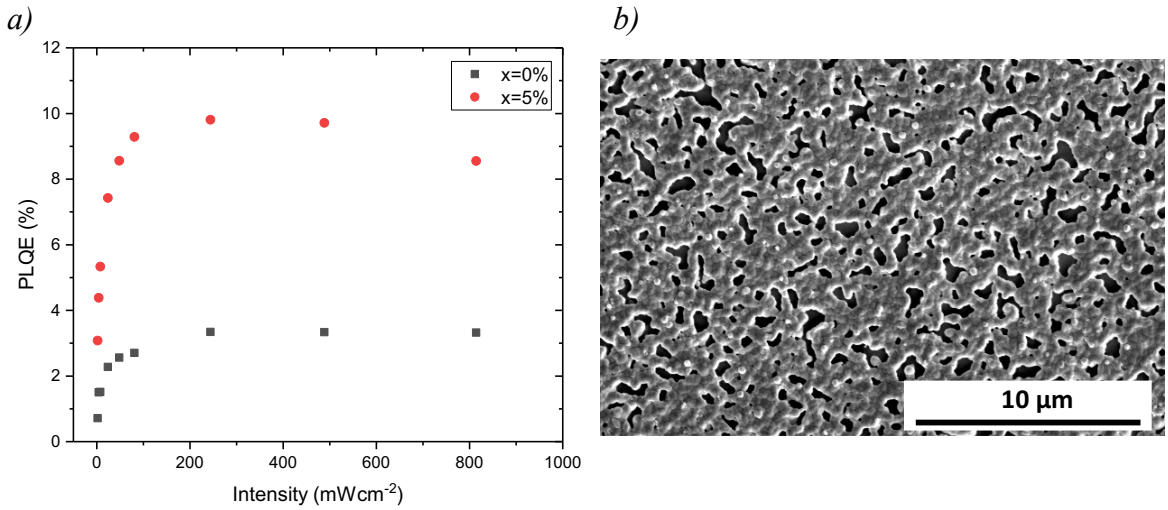

Figure S2. a) Significantly higher PLQE values can be obtained due to forming films with large pinhole areas as shown in the SEM image in b). No attempt was made at maximising PLQE values without causing pinholes.

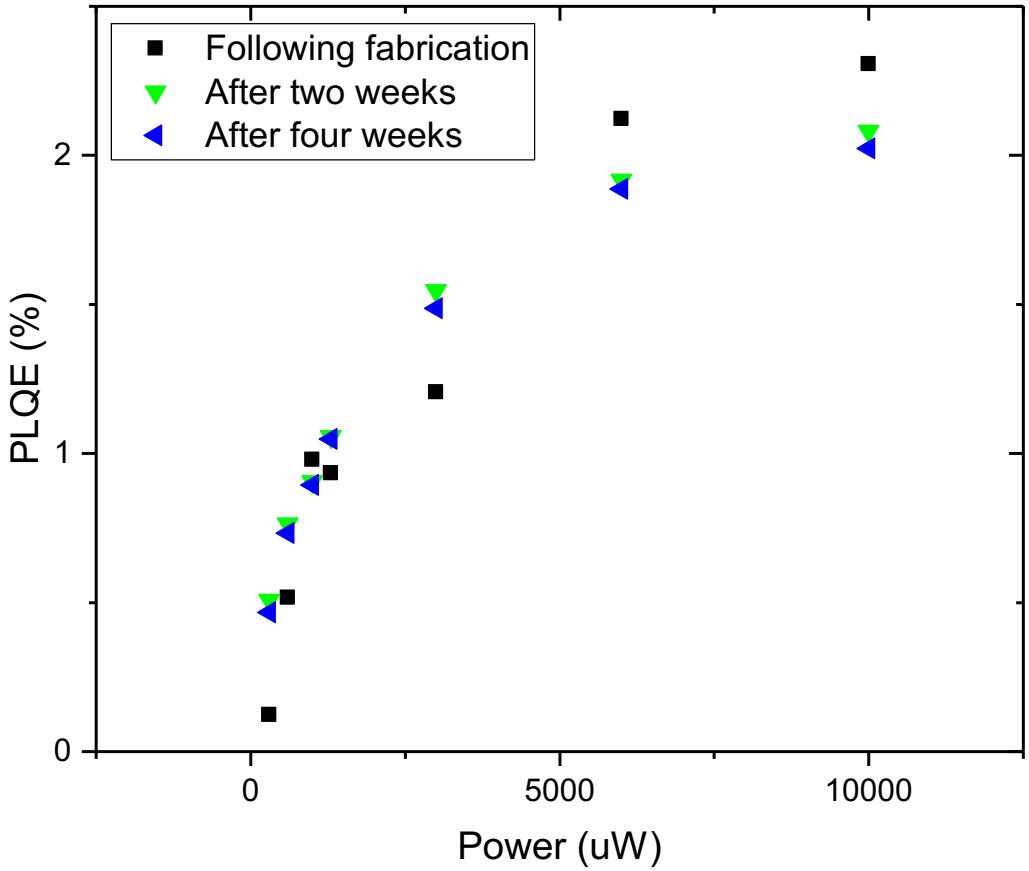

Figure S3. The PLQE value of encapsulated x=0 % films remains relatively stable over the course of four weeks.

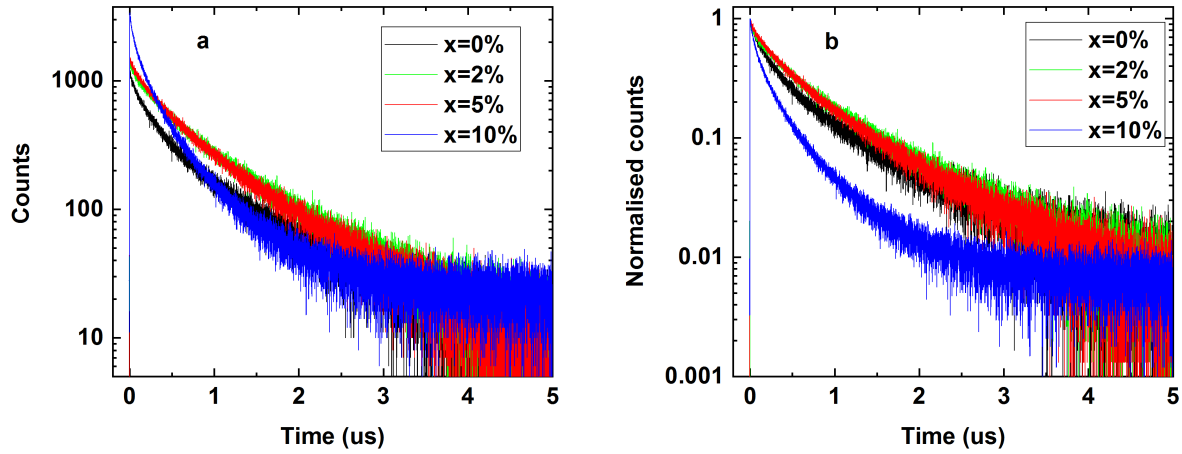

Figure S4. a) Unnormalised and b) normalised decay kinetics for all compositions.

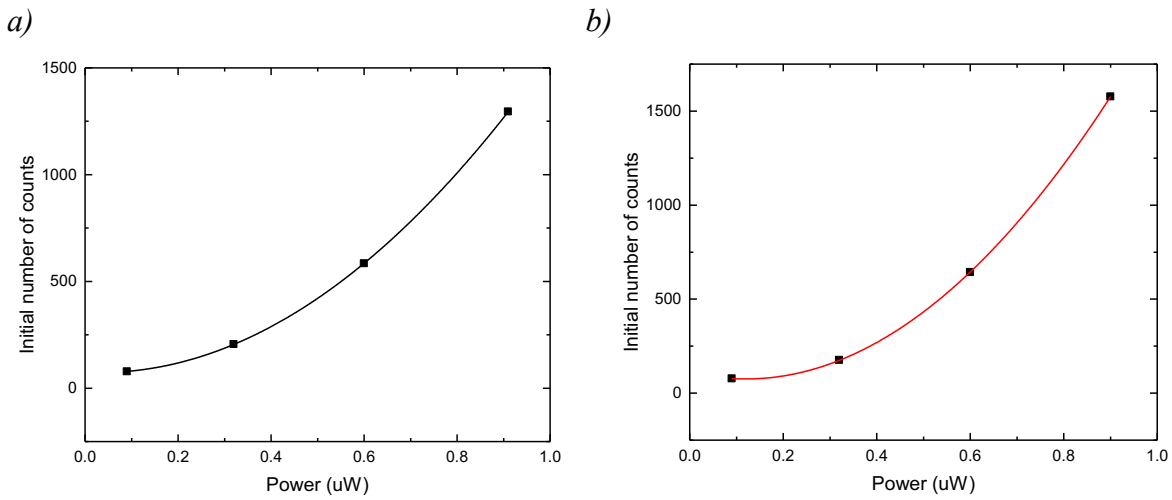

Figure S5. The scaling of initial TCSPC counts following photoexcitation with laser power is shown for x=0 % (a) and x=5 % (b). In both cases the relationship is observed to be quadratic (as per fitting), while the laser we used could not access low enough fluences to significantly explore any linear radiative regime.

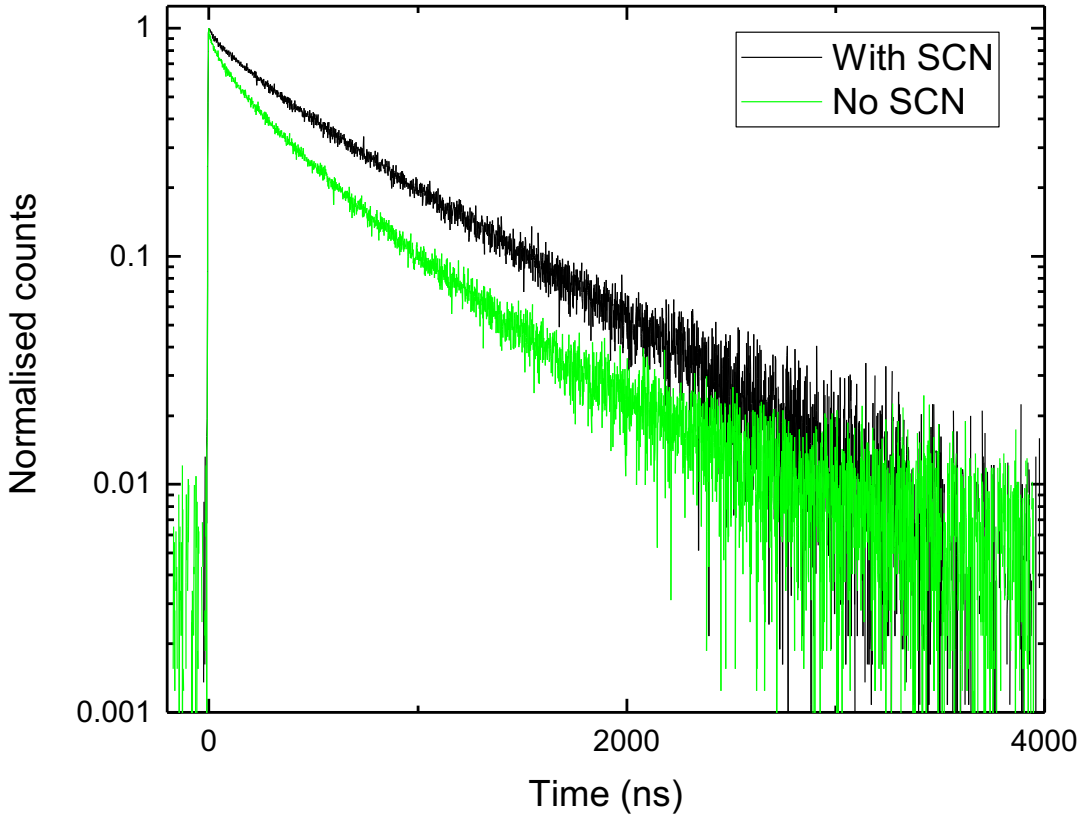

Figure S6. Films fabricated with Lead Thiocyanate (SCN) in the precursor solution have a longer lifetime, as measured by TCSPC.

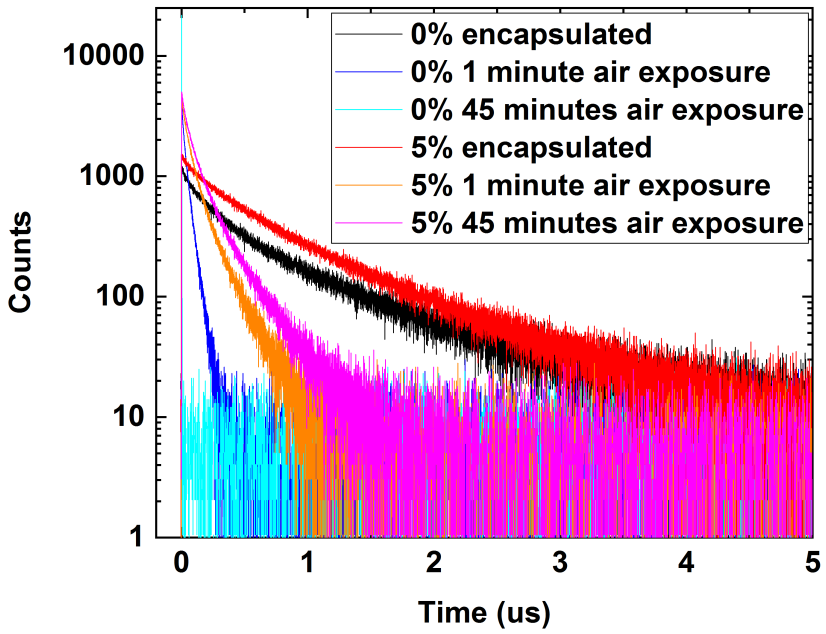

Figure S7. Unnormalised decays of those presented in main text Figure 1c and 1d.

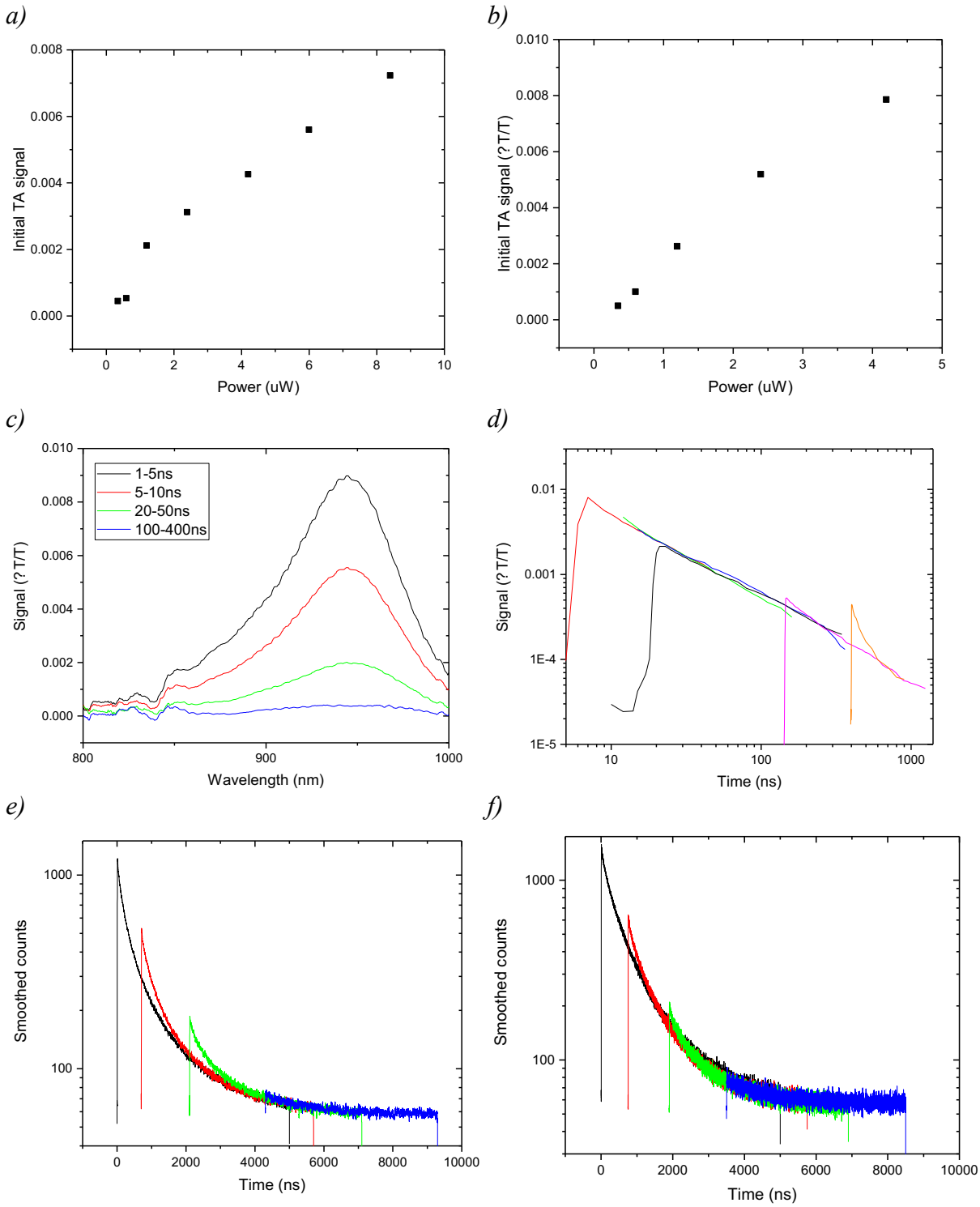

Figure S8. a) and b) demonstrate that the TA signal integrated about the ground state bleach at time 0 scales linearly with the power of the pulse beam for both x=0 % and x=5 % films respectively. c) shows the ground state bleached at different times following excitation for x=0 % (N.B. this excitation produces a carrier density of 10^{18} cm^{-3} hence the faster signal decay). d) Demonstrates the overlap of TA decay kinetics: by shifting time 0 the different fluences can be made to overlap, except at low excitation density where there is some 'history dependant' part in the TA spectra. This lack of overlap at short times is also observed in TCSPC spectra, as shown for x=0 % in e). We note that this history dependant part is reduced for x=5 %, as shown in f). As the Zinc containing films are more uniform, we

attribute this initial fast decay to charges exploring the energy landscape and finding the lowest energy sites. A discussion on similar observations in Cu(InGa)Se_2 films can be found in C. J. Hages et al.[9]

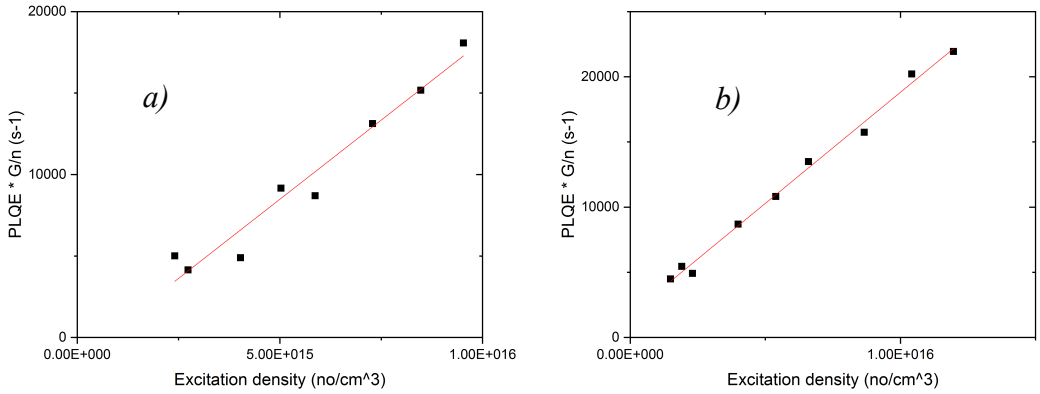

Figure S9. Fitting of PLQE data to extract a doping density as discussed in SI Note 3 for x=0 % and x=5 % in a) and b) respectively. Results are summarised in SI table 2.

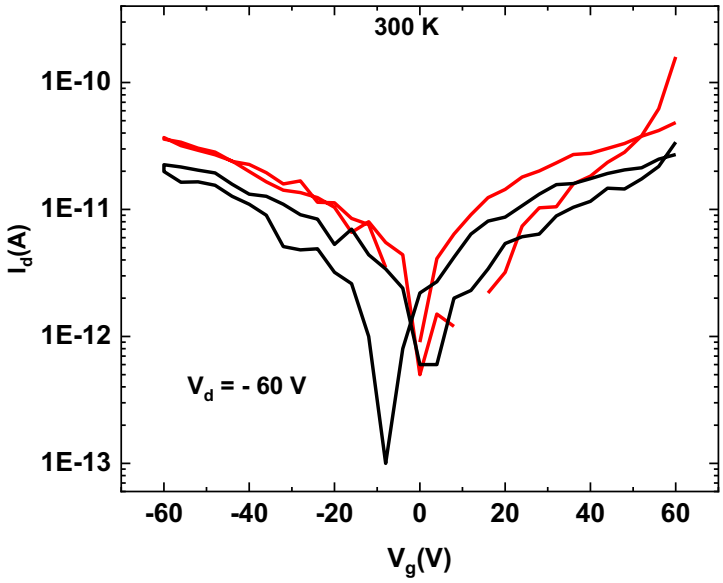

Figure S10. No transistor behaviour is observed for FET devices fabricated with a ZnI_2 thin film as the active layer.

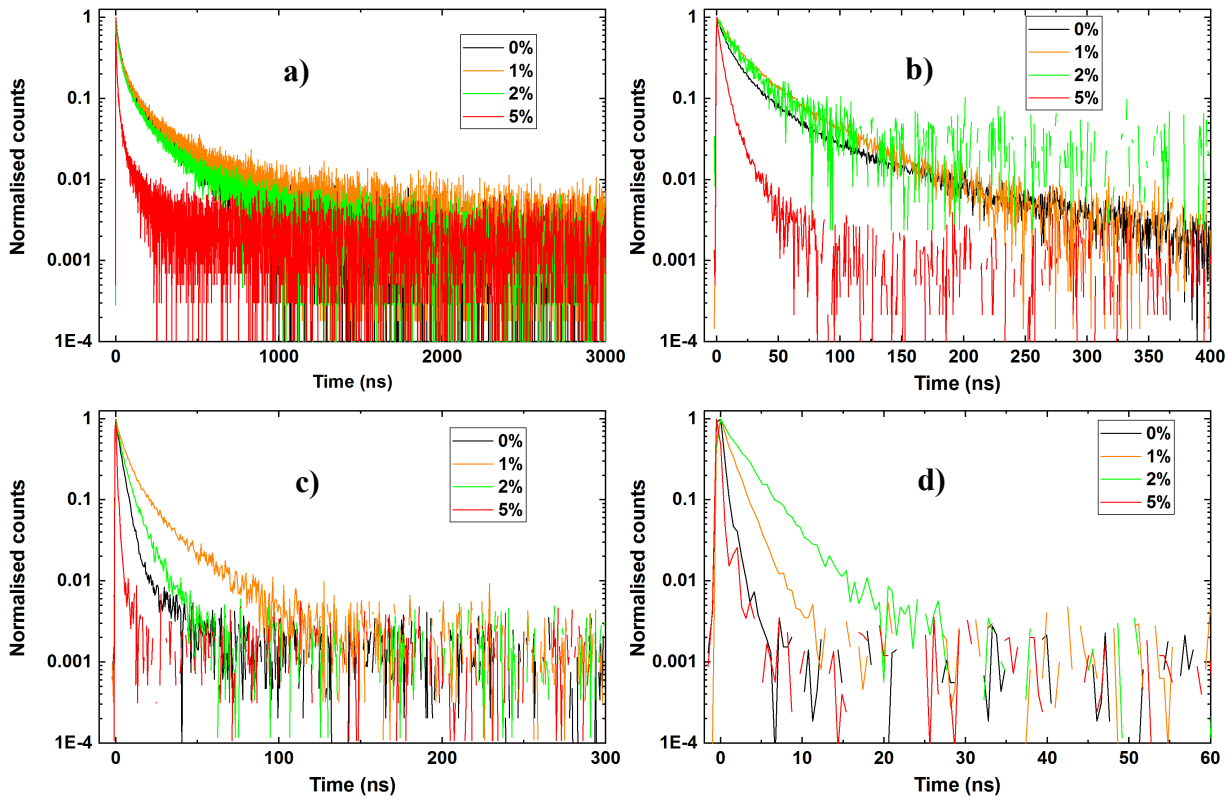

Figure S11. TCSPC decay of solvent quenched x=0 % to 5 % samples encapsulated, a), immediately following air exposure, b), following 30 minutes of air exposure, c), and following 50 minutes of air exposure, d). We note that the x=5 % sample shown here was anomalous and other x=5 % samples had the same lifetime as other samples shown in a) (but were not exposed to air).

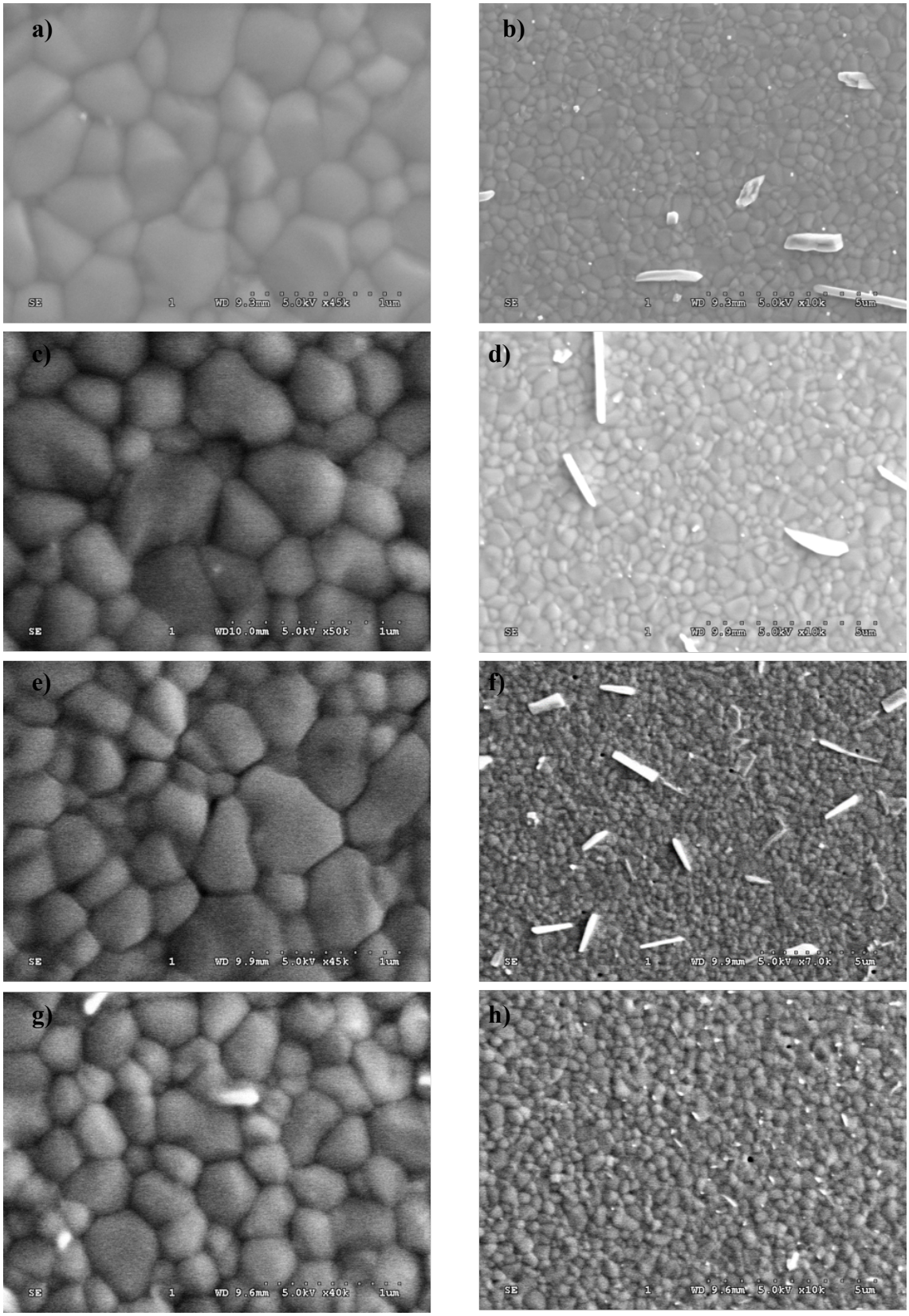

Figure S12. SEM images of x=0 % (a and b), x=1 % (c and d), x=2 % (e and f) and x=5 % (g and h) films spun via the antisolvent method. Grains are a comparable size in all cases and some small pinholes are introduced at higher x values. The white regions in visible in the right hand side images are thought to be associated with the presence of lead thiocyanate.

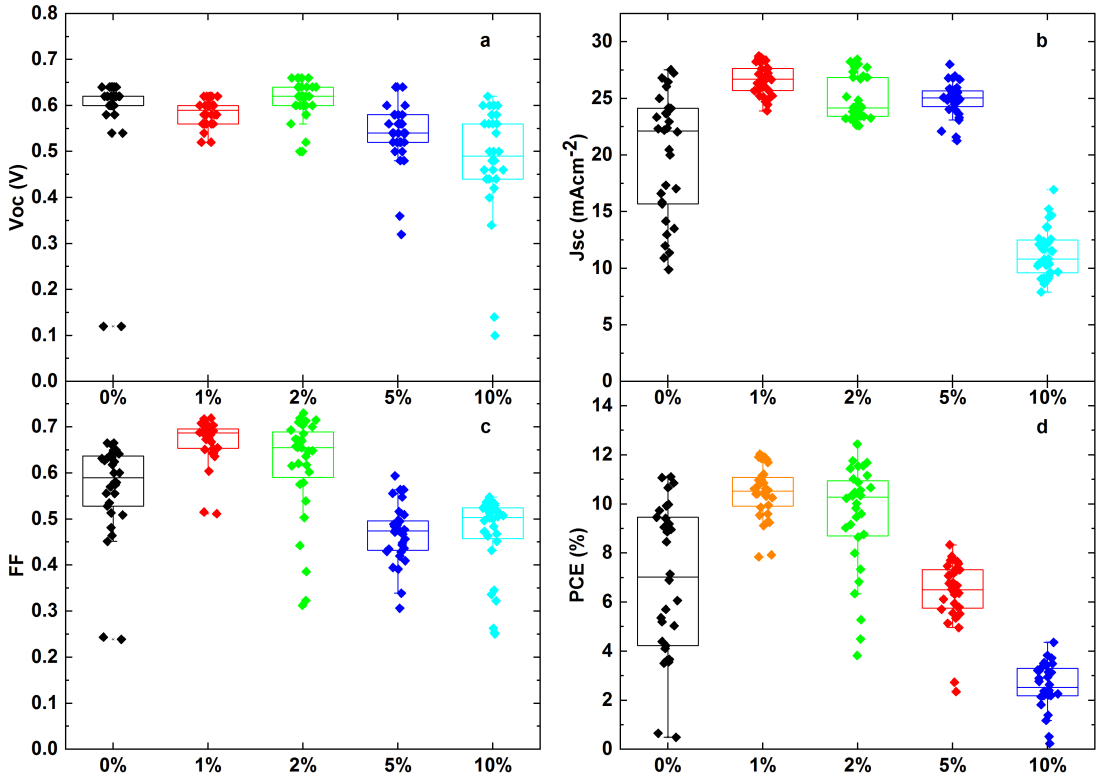

Figure S13. Performance of x=0-10 % solar cells two days after fabrication (following storage in a nitrogen filled glovebox and 2.5 hours of air exposure). V_{oc}, J_{sc}, FF and PCE are shown in a) to d) respectively.

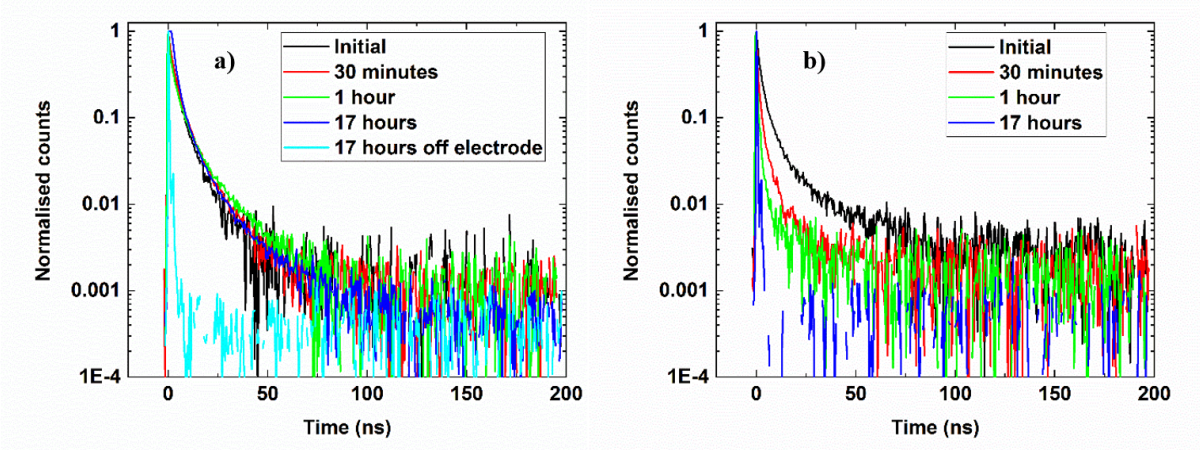

Figure S14. TCSPC decay curves of perovskite emission from the stack glass/perovskite(x=0 %)/PCBM/BCP with (a) and without (b) a silver electrode capping the stack following different amounts of air exposure. In a) 'off electrode' corresponds to a region of the same device stack which was not covered by silver due to being under the mask during evaporation. Samples were stored in a desiccator between measurements and measurement parameters are the same as reported in the main text.

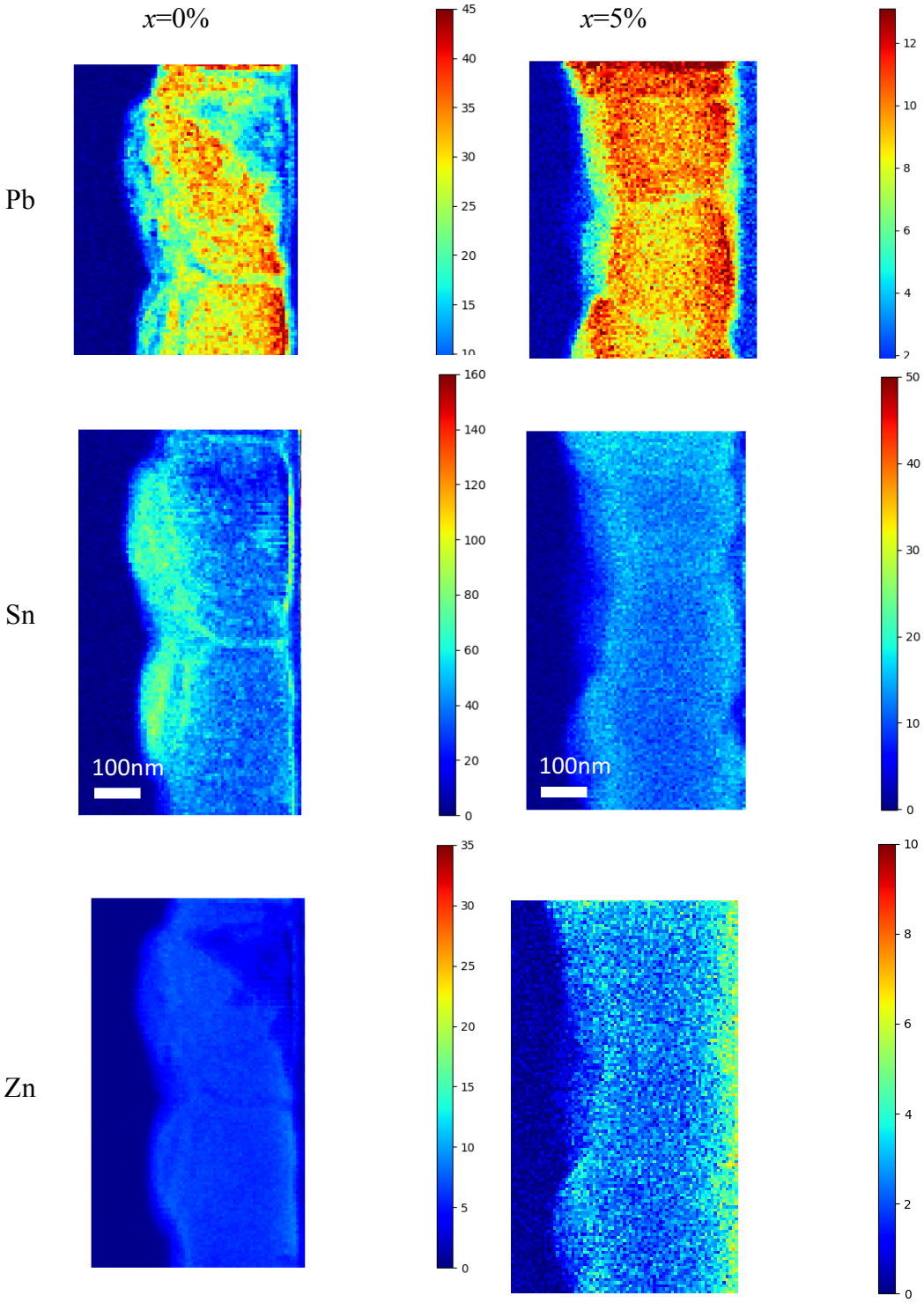

Figure S15. STEM/EDX results for films spun on PEDOT. Zn is still mainly distributed on the substrate side (right hand side of images). All scale bars are in arbitrary units.

a)

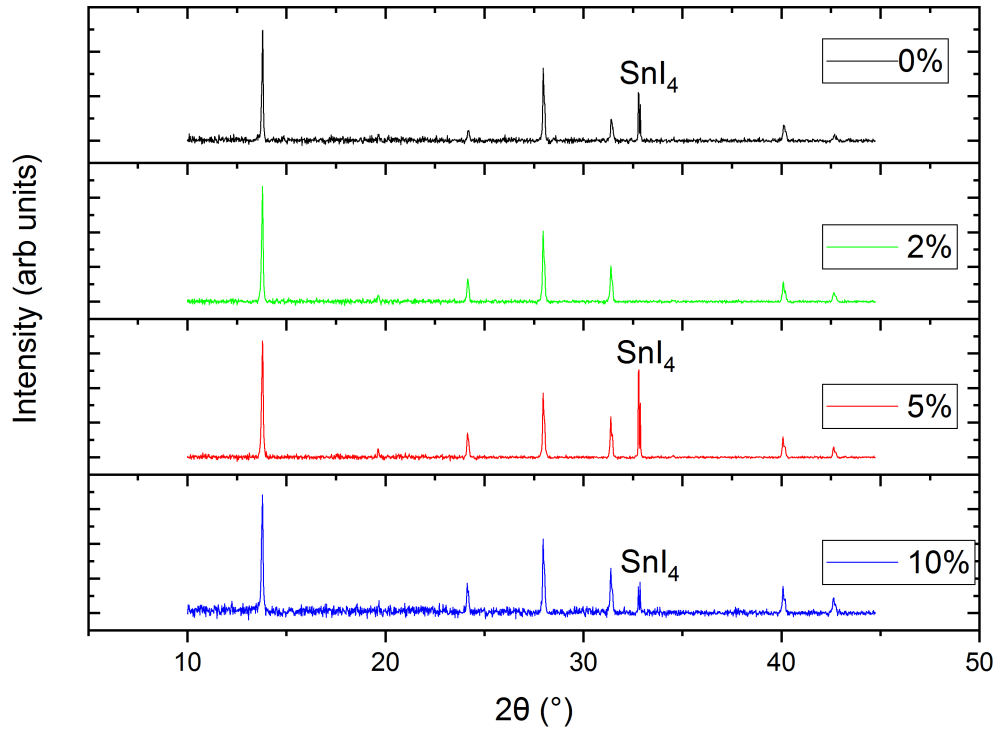

b)

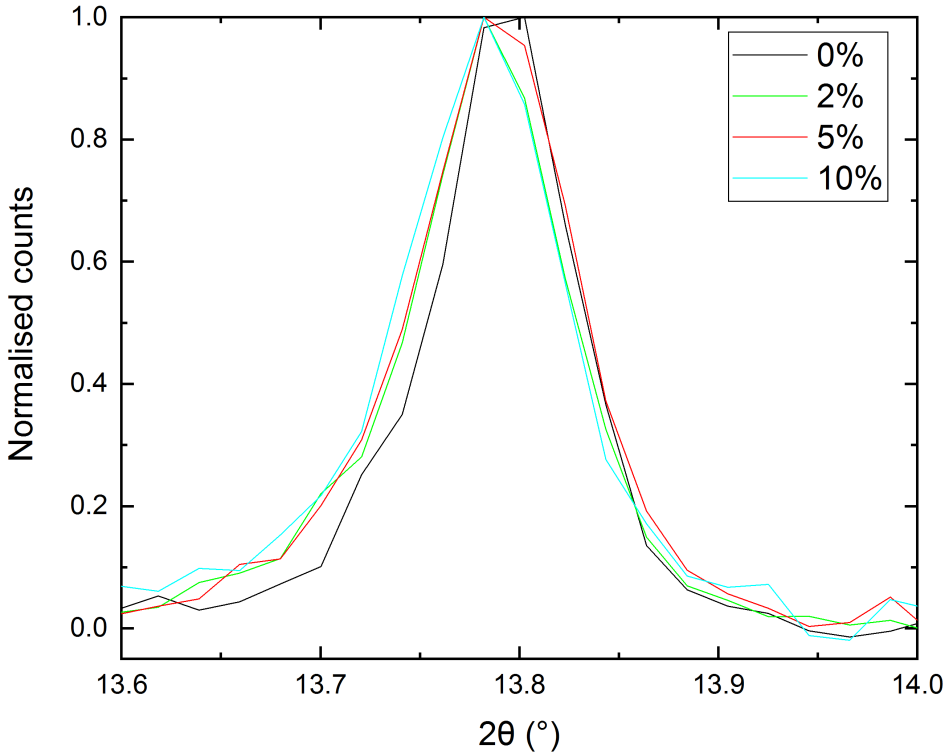

Figure S16. a) XRD data for all four films, taken on samples deposited on Silicon as measured in a Nitrogen atmosphere. All peaks except that at 33° could be assigned to a Pm3m lattice. The peak at 33°, which was present in all films except x=2 %, was assigned to SnI_4 P23, as marked on plots. We suggest that this peak is due to some residual Tin following fabrication and, while a contaminant, does not significantly influence the properties of the film. b) An example of a peak shift zoomed in.

Supplementary References

(1) De Mello, J. C.; Wittmann, H. F.; Friend, R. H. An Improved Experimental Determination of External Photoluminescence Quantum Efficiency. *Adv. Mater.* **1997**, *9* (3), 230–232. https://doi.org/10.1002/adma.19970090308.

(2) Skinner, D. R.; Whitcher, R. E. Measurement of the Radius of a High-Power Laser Beam near the Focus of a Lens. *J. Phys. E.* **1972**, *5* (3), 237–238. https://doi.org/10.1088/0022-3735/5/3/015.

(3) Rao, A.; Wilson, M. W. B.; Hodgkiss, J.; Albert-Seifried, S.; Bassler, H.; Friend, R. H. Exciton Fission and Charge Generation via Triplet Excitons in Pentacene/C60 Bilayers. *J. Am. Chem. Soc.* **2010**, No. 132, 12698–12703. https://doi.org/10.1021/nl102122x.

(4) HyperSpy 10.5281/zenodo.3352325. https://doi.org/10.5281/zenodo.3352325.

(5) Coelho, A. A.; Evans, J.; Evans, I.; Kern, A.; Parsons, S. The TOPAS Symbolic Computation System. *Powder Diffr.* **2011**, *26* (S1), S22–S25. https://doi.org/10.1154/1.3661087.

(6) Le Bail, A.; Duroy, H.; Fourquet, J. L. Ab-Initio Structure Determination of LiSbWO6 by X-Ray Powder Diffraction. *Mater. Res. Bull.* **1988**, *23* (3), 447–452.

(7) Stern, F. *Solid State Physics*; Seitz, F., Turnbull, D., Eds.; Academic Press Inc.: New York and London, 1963. https://doi.org/10.1016/S0081-1947(08)60594-9.

(8) Richter, J. M.; Abdi-Jalebi, M.; Sadhanala, A.; Tabachnyk, M.; Rivett, J. P. H.; Pazos-Outón, L. M.; Gödel, K. C.; Price, M.; Deschler, F.; Friend, R. H. Enhancing Photoluminescence Yields in Lead Halide Perovskites by Photon Recycling and Light Out-Coupling. *Nat. Commun.* **2016**, *7*, 13941. https://doi.org/10.1038/ncomms13941.

(9) Hages, C. J.; Redinger, A.; Levcenko, S.; Hempel, H.; Koeper, M. J.; Agrawal, R.; Greiner, D.; Kaufmann, C. A.; Unold, T. Identifying the Real Minority Carrier Lifetime in Nonideal Semiconductors: A Case Study of Kesterite Materials. *Adv. Energy Mater.* **2017**, *7* (18), 1–10. https://doi.org/10.1002/aenm.201700167.